Published in Proceedings of the 6th International Symposium on Experimental Robotics, Sydney, March 26-28

Identification of Joint Elasticity of Industrial Robots

G.E. Hovland[†], E. Berglund[*] and O.J. Sørdalen[†]

[†]ABB Corporate Research,
Information Technology and Control Systems Division,
Bergerveien 12, N-1375 Billingstad, Norway.
E-mail: {geir.hovland,ole.sordalen}@nocrc.abb.no

[*]Department of Engineering Cybernetics,
The Norwegian University of Science and Technology,
N-7034 Trondheim, Norway.
E-mail: Einar.Berglund@itk.ntnu.no

Abstract: *In this paper we present a new method for the identification of joint elasticities of industrial robots. The presented method is able to identify the elasticity parameters in presence of coupled dynamics between two joints. An accurate model description of the joint elasticities is absolutely necessary to achieve accurate path tracking of industrial robots at high speeds. The industrial requirements for path accuracy in applications such as spray painting, waterjet cutting and assembly are so high that elasticity effects have to be accounted for by the control system.*

1. Introduction

The modelling of modern robot systems as rigid mechanical systems is an unrealistic simplification. The industrial requirements for path accuracy in applications such as spray painting, waterjet cutting, plasma cutting and assembly are so high that elasticity effects have to be accounted for by the control system. There are two sources of vibration in robot manipulators: 1) joint elasticity, due to the elasticity of motion transmission elements such as harmonic drives, gear-boxes, belts or long shafts [8], and 2) link elasticity, introduced by a long reach and slender/lightweight construction of the arm, [1, 5].

Many industrial robot systems use elastic transmission elements which introduce joint elasticity. Given a dynamic model description including the rigid-body dynamics and joint elasticity, several control algorithms have been proposed in the literature, see for example [2] for a survey. To be able to implement such control algorithms and achieve the strict path tracking requirements from industry, one needs very accurate parameter estimates of the stiffness and damping constants of the transmission elements.

In this paper we present a new approach to the identification problem of joint elasticity. The proposed solution assumes that the rigid-body dynamics are known. For a rigid-body dynamics identification method, see for example the work by [9]. We show that when the rigid-body dynamics are known the joint elasticity identification becomes a linear problem. The linear formulation avoids the problems associated with non-linear estimation techniques, such as proper selection of initial values and convergence. Another advantage of the method presented in this paper is the little amount of measurement data required. In principle, only one sinoid measurement series is required to identify four elasticity parameters (spring and damper constants for two coupled joints). To increase the accuracy of the estimated parameters, additional measurement series can easily be utilised.

Most industrial robots do not have any velocity or acceleration sensors. Instead, the velocity and acceleration measurements are normally generated by numerical differentiation. In this paper we present a different approach where the position measurements are approximated by Fourier coefficients and the velocity and acceleration data are found analytically. The approach used in our paper avoids the troublesome noise problems associated with numerical differentiation.

The problem of controlling robots with joint elasticities has received a significant amount of attention in the literature, see for example [3, 4, 6, 10]. The identification problem, however, has received less attention. The work by De Luca, for example, assumes that the joint elasticity parameters are known and the elasticity parameters are used directly in the design of the control laws. Hence, the methods and results presented in our paper will be directly beneficial to several of the existing control strategies in the literature.

2. Model of Joint Dynamics

Figure 1 presents a simplified illustration of a robot with two elastic joints with coupled dynamics. The elasticity model of these joints with coupled inertia terms is shown in Figure 2. The goal of the identification algorithm is to identify K_1, D_1, K_2 and D_2 when the rigid-body inertia parameters J_{m1}, J_{m2}, J_{a1}, J_{a2}, J_{12} and J_{21} are known. The equations of motion are given by

$$\begin{aligned}
&J_{m1}\ddot{\theta}_{m1} + D_1(\dot{\theta}_{m1} - \dot{\theta}_{a1}) + K_1(\theta_{m1} - \theta_{a1}) = \tau_{m1} \\
&J_{a1}\ddot{\theta}_{a1} + J_{12}\ddot{\theta}_{a2} + D_1(\dot{\theta}_{a1} - \dot{\theta}_{m1}) + K_1(\theta_{a1} - \theta_{m1}) = 0 \\
&J_{m2}\ddot{\theta}_{m2} + D_2(\dot{\theta}_{m2} - \dot{\theta}_{a2}) + K_2(\theta_{m2} - \theta_{a2}) = \tau_{m2} \\
&J_{a2}\ddot{\theta}_{a2} + J_{21}\ddot{\theta}_{a1} + D_2(\dot{\theta}_{a2} - \dot{\theta}_{m2}) + K_2(\theta_{a2} - \theta_{m2}) = 0
\end{aligned} \tag{1}$$

Note that the set of equations (1) do not contain any velocity dependent coupling terms, such as Coriolis or centripetal forces. The main reason why we have excluded these terms, is to make the system linear in all state variables $(\theta_{m1}, \dot{\theta}_{m1})$, $(\theta_{a1}, \dot{\theta}_{a1})$, $(\theta_{m2}, \dot{\theta}_{m2})$ and $(\theta_{a2}, \dot{\theta}_{a2})$. The Coriolis and Centripetal forces contain nonlinear terms such as $\dot{\theta}_{a1}\dot{\theta}_{a2}$ and $\dot{\theta}_{a1}^2$.

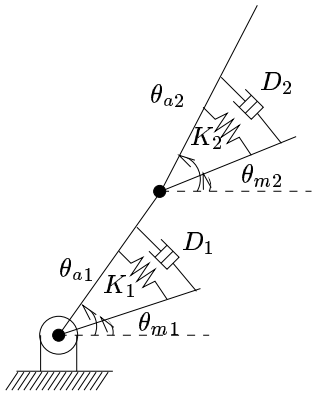

Figure 1. *Visualisation of robot with two dynamically coupled joints and joint elasticities. The differences between the motor variables θ_m and the arm variables θ_a are exaggerated to illustrate the elasticity parameters.*

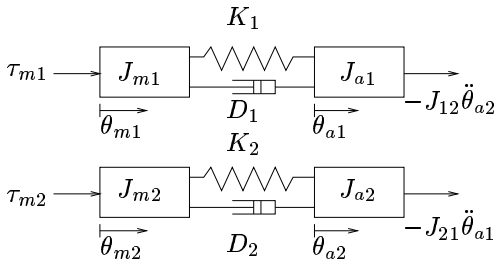

Figure 2. *Two-mass elastic model of two joints with coupled-inertia dynamics.*

A linear model significantly simplifies the identification algorithm and the model parameters can be found directly from a frequency response analysis. However, care should be taken when the motions of the robot joints are generated during the identification experiments to keep the velocity terms as low as possible.

3. Identification Algorithm

In this section we present the three steps of the identification algorithm; in 3.1 the generation of Fourier coefficients from a sinoid excitation of the robot joints and in 3.2 the identification of the model parameters.

3.1. Fourier Coefficients

Let $f(t)$ be a measurement signal, either joint position or joint torque. In the experiments these signals are generated as sinoid functions. Hence, to remove the effects from measurements noise, friction and other nonlinear terms, we approximate the measurement $f(t)$ by a pure sinoid function using Fourier coefficients given by

$$\begin{aligned} a &= \frac{1}{L/2}\int_0^L (f(t)\sin(\omega t))\,dt \\ b &= \frac{1}{L/2}\int_0^L (f(t)\cos(\omega t))\,dt \end{aligned} \qquad (2)$$

where ω is the natural frequency of the generated measurement series and L is an integer number times the period of sinoid. L should be chosen larger than one period to achieve time averaging of the data and further reduce the effects of noise and nonlinearities.

Finally, a complex number representation of the sinoid measurement is given by

$$y = a + ib \tag{3}$$

The complex number y contains both amplitude and phase information and will be used in the next section to find the transfer function matrix. Given the complex number y for the position measurements, the velocities and accelerations are found analytically, ie.

$$\begin{aligned} \theta &= a + ib \\ \dot{\theta} &= \theta(i\omega) \\ \ddot{\theta} &= \theta(i\omega)^2 \end{aligned} \tag{4}$$

where ω is the known excitation frequency in (rad/sec). In the experiments, the Fourier coefficients are found for several different frequencies ω in the robot's bandwidth. The analytical generation of the velocity and acceleration signals is a major advantage. For most robot systems, only joint position measurements are available from encoder data. By differentiation the encoder data twice, a large amount of quantization noise is introduced in the acceleration data. The analytical generation of velocity and acceleration from sinoid functions avoids the quantization noise problem. By time-averaging over a large number of periods (L large), the influence from quantization noise in the velocity and acceleration estimates is neglectable.

3.2. Identification of Model Parameters

First, we write the system equations (1) on vector form.

$$\mathbf{M}s^2\mathbf{q} + \mathbf{D}s(\mathbf{q} - \mathbf{q_a}) + \mathbf{K}(\mathbf{q} - \mathbf{q_a}) = \tau \tag{5}$$

$$\mathbf{M}_2 s^2\mathbf{q_a} + \mathbf{D}s(\mathbf{q_a} - \mathbf{q}) + \mathbf{K}(\mathbf{q_a} - \mathbf{q}) = \mathbf{0} \tag{6}$$

where s is the Laplace transform. The matrices and vectors are given by

$$\begin{aligned} \mathbf{q} &= \begin{bmatrix} \theta_{m1} \\ \theta_{m2} \end{bmatrix}, \quad \mathbf{q_a} = \begin{bmatrix} \theta_{a1} \\ \theta_{a2} \end{bmatrix}, \quad \tau = \begin{bmatrix} \tau_{m1} \\ \tau_{m2} \end{bmatrix} \\ \mathbf{M} &= \begin{bmatrix} J_{m1} & 0 \\ 0 & J_{m2} \end{bmatrix}, \quad \mathbf{M}_2 = \begin{bmatrix} J_{a1} & J_{12} \\ J_{21} & J_{a2} \end{bmatrix} \\ \mathbf{D} &= \begin{bmatrix} D_1 & 0 \\ 0 & D_2 \end{bmatrix}, \quad \mathbf{K} = \begin{bmatrix} K_1 & 0 \\ 0 & K_2 \end{bmatrix} \end{aligned} \tag{7}$$

By substitution of equation (6) into equation (5) the motor dynamics can be written on the following linear form in $\mathbf{D}$ and $\mathbf{K}$.

$$\mathbf{D}[(\mathbf{I} + \mathbf{M}_2^{-1}\mathbf{M})s^3\mathbf{q} - \mathbf{M}_2^{-1}s\tau] + \mathbf{K}[(\mathbf{I} + \mathbf{M}_2^{-1}\mathbf{M})s^2\mathbf{q} - \mathbf{M}_2^{-1}\tau] = s^2\tau - \mathbf{M}s^4\mathbf{q} \tag{8}$$

From the Fourier coefficients of $\mathbf{q}$ and τ, we generate the following vectors.

$$\begin{bmatrix} a_1 \\ a_2 \end{bmatrix} = (\mathbf{I} + \mathbf{M}_2^{-1}\mathbf{M})s^2\mathbf{q} - \mathbf{M}_2^{-1}\tau \tag{9}$$

$$\begin{bmatrix} a_3 \\ a_4 \end{bmatrix} = (\mathbf{I} + \mathbf{M}_2^{-1}\mathbf{M})s^3\mathbf{q} - \mathbf{M}_2^{-1}s\tau = i\omega \begin{bmatrix} a_1 \\ a_2 \end{bmatrix} \tag{10}$$

$$\begin{bmatrix} b_1 \\ b_2 \end{bmatrix} = s^2\tau - \mathbf{M}s^4\mathbf{q} \tag{11}$$

We then have

$$\begin{aligned}
\mathbf{A} &= \begin{bmatrix} \Re(i\omega a_1) & \Re(a_1) & 0 & 0 \\ \Im(i\omega a_1) & \Im(a_1) & 0 & 0 \\ 0 & 0 & \Re(i\omega a_2) & \Re(a_2) \\ 0 & 0 & \Im(i\omega a_2) & \Im(a_2) \end{bmatrix} \\
&= \begin{bmatrix} -\omega\Im(a_1) & \Re(a_1) & 0 & 0 \\ \omega\Re(a_1) & \Im(a_1) & 0 & 0 \\ 0 & 0 & -\omega\Im(a_2) & \Re(a_2) \\ 0 & 0 & \omega\Re(a_2) & \Im(a_2) \end{bmatrix} \\
\mathbf{b} &= \begin{bmatrix} \Re(b_1) \\ \Im(b_1) \\ \Re(b_2) \\ \Im(b_2) \end{bmatrix}, \quad \mathbf{p} = \begin{bmatrix} D_1 \\ K_1 \\ D_2 \\ K_2 \end{bmatrix} \\
\mathbf{Ap} &= \mathbf{b}
\end{aligned} \tag{12}$$

The parameter vector $\mathbf{p}$ can be identified from only one sinoid measurement series when we use both the real and imaginary parts of the Fourier coefficients. To achieve a robust identification result, it is advisable to use several sinoid measurement series with different frequencies. The $\mathbf{A}$ matrix and the $\mathbf{b}$ vector will then have $4n$ rows, where n is the number of different frequencies. The parameter vector $\mathbf{p}$ is then simply found from the pseudo-inverse, ie.

$$\mathbf{p} = \mathbf{A}^+\mathbf{b} \tag{13}$$

$$\mathbf{A}^+ = (\mathbf{A}^T\mathbf{A})^{-1}\mathbf{A}^T \tag{14}$$

The pseudo-inverse is equal to a least-squares estimation method, see for example [7]. The explicit solutions for D_1, K_1, D_2 and K_2 found by solving equations (13)-(14) are given below.

$$\begin{aligned}
D_1 &= -\frac{\sum_{i=1}^n \Im(a_1)\Re(b_1) - \Re(a_1)\Im(b_1)}{\sum_{i=1}^n \omega_i(\Re(a_1)^2 + \Im(a_1)^2)} \\
K_1 &= \frac{\sum_{i=1}^n \Re(a_1)\Re(b_1) + \Im(a_1)\Im(b_1)}{\sum_{i=1}^n \Re(a_1)^2 + \Im(a_1)^2} \\
D_2 &= -\frac{\sum_{i=1}^n \Im(a_2)\Re(b_2) - \Re(a_2)\Im(b_2)}{\sum_{i=1}^n \omega_i(\Re(a_2)^2 + \Im(a_2)^2)}
\end{aligned}$$

$$K_2 = \frac{\sum_{i=1}^{n} \Re(a_2)\Re(b_2) + \Im(a_2)\Im(b_2)}{\sum_{i=1}^{n} \Re(a_2)^2 + \Im(a_2)^2} \tag{15}$$

where n is the number of frequencies.

4. Experiments

In this section we present the experimental results from the elasticity identification of an ABB robot used for waterjet cutting at a customer site in Sweden. We also present the direct improvements achieved in path tracking performance when using the identified elasticity parameters in the control structure.

Section 4.1 describes the non-parametric identification of the multivariable transfer function matrix. The elements in this matrix are used to verify the identification results. In section 4.2 we present the experimental results from the identification algorithm developed in section 3. Finally, in section 4.3 we present the improvements in path tracking performance for a waterjet cutting application.

4.1. Identification of Transfer Function Matrix

Only the motor state variables (θ_{m1}, $\dot{\theta}_{m1}$) and (θ_{m2}, $\dot{\theta}_{m2}$) can be measured and approximated by Fourier coefficients. Hence, for the identification of the model parameters we only use the 2×2 subsystem of equation (1) corresponding to the motor variables.

$$\begin{bmatrix} \ddot{\theta}_{m1} \\ \ddot{\theta}_{m2} \end{bmatrix} = \begin{bmatrix} H_{11} & H_{12} \\ H_{21} & H_{22} \end{bmatrix} \begin{bmatrix} \tau_{m1} \\ \tau_{m2} \end{bmatrix} \tag{16}$$

Let y_1 and y_3 be the complex numbers of $\ddot{\theta}_{m1}$ and $\ddot{\theta}_{m2}$ for one measurement series. Let τ_1 and τ_3 be the corresponding complex numbers for the joint torques τ_{m1} and τ_{m2}, respectively. Similarly, y_2, y_4, τ_2 and τ_4 describe a second measurement series. We then have

$$\begin{bmatrix} y_1 \\ y_2 \\ y_3 \\ y_4 \end{bmatrix} = \begin{bmatrix} \tau_1 & \tau_3 & 0 & 0 \\ \tau_2 & \tau_4 & 0 & 0 \\ 0 & 0 & \tau_1 & \tau_3 \\ 0 & 0 & \tau_2 & \tau_4 \end{bmatrix} \begin{bmatrix} H_{11}(i\omega) \\ H_{12}(i\omega) \\ H_{21}(i\omega) \\ H_{22}(i\omega) \end{bmatrix} \tag{17}$$

For each frequency ω, the four complex transfer function elements are simply found by inversion of the τ matrix, ie.

$$\begin{bmatrix} H_{11}(i\omega) \\ H_{12}(i\omega) \\ H_{21}(i\omega) \\ H_{22}(i\omega) \end{bmatrix} = \begin{bmatrix} \tau_1 & \tau_3 & 0 & 0 \\ \tau_2 & \tau_4 & 0 & 0 \\ 0 & 0 & \tau_1 & \tau_3 \\ 0 & 0 & \tau_2 & \tau_4 \end{bmatrix}^{-1} \begin{bmatrix} y_1 \\ y_2 \\ y_3 \\ y_4 \end{bmatrix} \tag{18}$$

To identify the entire transfer function matrix H, two measurement series generating sinoid functions in $\ddot{\theta}_{m1}$ and $\ddot{\theta}_{m2}$ are required for several frequencies ω within the joint bandwidths.

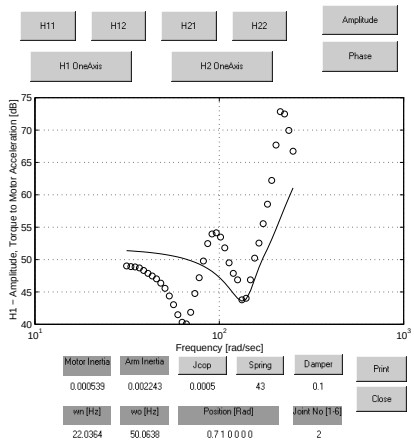

Figure 3. *Measured transfer function* $|H_{11}(i\omega) + H_{12}(i\omega)\frac{\tau_{m2}}{\tau_{m1}}|$ *(dotted) and model* $|\frac{\ddot{\theta}_{m1}}{\tau_{m1}}|$ *(solid) with estimated elasticity parameters* $D_1 = 0.10$, $K_1 = 43.0$, $D_2 = 0.015$ *and* $K_2 = 7.5$.

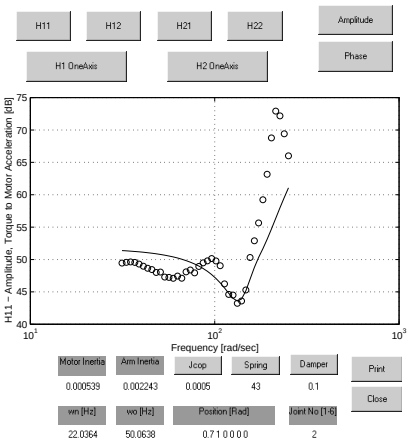

Figure 4. *Estimated transfer function* $|H_{11}(i\omega)|$ *(dotted) and model* $|\frac{\ddot{\theta}_{m1}}{\tau_{m1}}|$ *(solid) with estimated elasticity parameters* $D_1 = 0.10$, $K_1 = 43.0$, $D_2 = 0.015$ *and* $K_2 = 7.5$.

4.2. Identification of Elasticity Parameters

In Figure 3 the dotted curve shows the measured transfer function from motor torque to motor acceleration. During the experiments, the controller loops on all the joints are activated which is necessary to prevent the manipulator from collapsing due to the gravity torque. Note that two resonance modes are visible in the transfer function in Figure 3. One of these resonance modes is caused by the dynamic inertia coupling between the joints and the controller loop of the coupled joint. Hence, to identify the spring and damper constants directly from the measurements of Figure 3 is difficult.

The dotted curves in the Figures 4 and 5 show the estimated transfer functions H_{11} and H_{22} found using equation (18). Notice that these two transfer functions both have only one dominating resonance mode. The four elasticity parameters $K_1 = 43.0$, $K_2 = 7.5$, $D_1 = 0.10$ and $D_2 = 0.015$ were estimated using the method described in equations (5)–(15) when all the inertia parameters $\mathbf{M}$ and $\mathbf{M}_2$ were known.

To verify that the estimated results correspond to the estimated transfer functions H_{11} and H_{22} from section 4.3, we have plotted the model (solid curve) in all the Figures 3–5. We see from Figure 3 that the resonance mode caused by the joint elasticity, corresponds to the second elasticity mode in the measured transfer function. Figures 4 and 5 show that the identified model given K_1, K_2, D_1 and D_2 match the estimated transfer functions H_{11} and H_{22} well. We believe that the differences in the Figures are caused by unmodelled dynamics, such as the nonlinear velocity terms or joint friction.

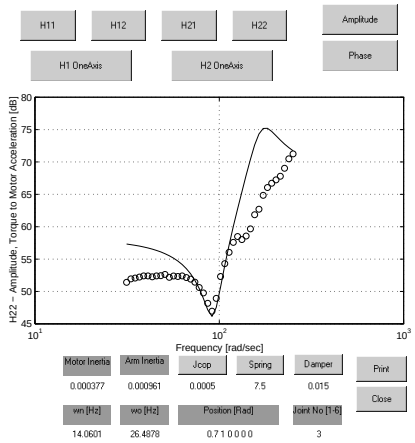

Figure 5. *Estimated transfer function* $|H_{22}(i\omega)|$ *(dotted) and model* $|\frac{\ddot{\theta}_{m2}}{\tau_{m2}}|$ *(solid) with estimated elasticity parameters* $D_1 = 0.10$, $K_1 = 43.0$, $D_2 = 0.015$ *and* $K_2 = 7.5$.

Figure 6. *Experimental setup consisting of a Waterjet cutting cell and an ABB robot.*

4.3. Waterjet Cutting Application

To demonstrate the importance of accurate estimates of the elasticity parameters, we present results from tests in a waterjet cutting cell from ABB I-R Waterjet Systems in Sweden. ABB I-R is a global leader in sophisticated three-dimensional robotized waterjet cutting systems for trimming and finishing components in general manufacturing and the automobile industry. The company is also a leading manufacturer of cutting tables and associated systems for two-dimensional waterjet cutting. Waterjet cutting is used in a wide range of industries: interior finish on vehicles, aerospace manufacture, metal fabrication, stone cutting, textile industries, automotive and truck manufacture, sheet metal industries, plastic processing, architectural metal and glass cutting and food processing. The path tracking requirements for finished products are extremely high. Using manipulators with elastic joints, the requirements from industry can only be satisfied with accurate estimates of the elasticity parameters.

The cutting cell is shown in Figure 6, where an ABB robot is mounted in the ceiling and the cutting is performed in the horizontal plane in a $1mm$ thick plastic material. Figure 7 shows the outlines of the cutting paths. The squares have dimension $28mm \times 45mm$. The Cartesian cutting speed was chosen $300mm/sec$. The three shapes at the top of the figure were cut with a non-optimal choice of elasticity parameters in the servo controllers. The right-most figure has the largest corner zones and an oscillatory behaviour is clearly visible. In fact, the largest path tracking error for this particular test was several millimeters. The three shapes at the bottom of the figure show the same tests when using the identified elasticity parameters in the control

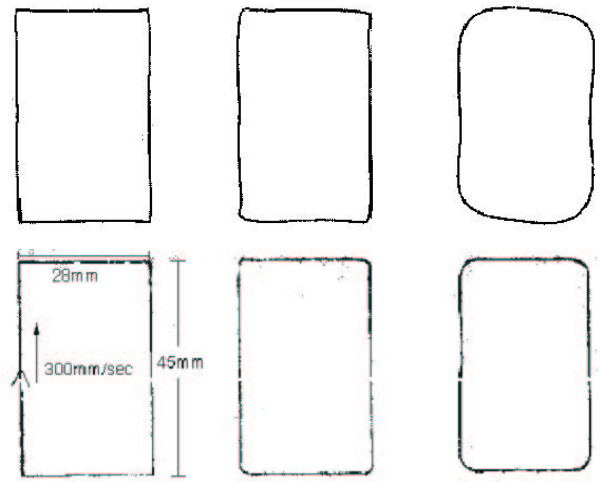

Figure 7. *Top: Cutting path with non-optimised elasticity parameters. Bottom: Cutting path with identified elasticity parameters.*

structure. This time the oscillatory behaviour is significantly reduced. With the identified elasticity parameters, the path tracking performance of the ABB I-R Waterjet cell is well inside the requirements for the industrial waterjet cutting applications mentioned above.

5. Conclusions

In this paper we have presented a new approach to the identification of joint elasticities between two robot joints with coupled dynamics. The main advantage of the method is the linear problem formulation in the elasticity parameters (joint stiffness and damping). The linear formulation allows for a straightforward estimation of the parameters using a weighted least squares approach. Hence, typical problems associated with non-linear estimation techniques, such as convergence problems and proper selection of initial parameter values are avoided.

The results show that the identification method is able to compute accurate parameter estimates with a good match between the identified model and measured transfer function responses. The identified elasticity parameters can be used directly in the control structure to achieve accurate path tracking performance at high speeds of industrial robots.

The method has been tested in a waterjet cutting application. When using the identified elasticity parameters, the waterjet cutting cell is able to meet strict industrial requirements with large cutting velocities.

References

[1] Book W.J. (1988): "Modelling, design, and control of flexible manipulator arms: A tutorial review", *Proceedings of the 29th IEEE Conference on Decision and Control*, Honolulu, HI, pp.500-506.

[2] De Luca A. (1998a): "Trajectory Control of Flexible Manipulators", *Control Problems in Robotics and Automation*, pp. 83-104, Editors: B. Siciliano and K.P. Valavanis, Springer.

[3] De Luca A. (1988b): "Dynamic Control of Robots with Joint Elasticity", *Proceedings of the 29th IEEE Conference on Decision and Control*, Honolulu, HI, pp.500-506.

[4] De Luca A. (1988c): "Control Properties of Robot Arms with Joint Elasticity", In: Byrnes C.I., Martin C.F., Saeks R.E. (eds), *Analysis and Control of Nonlinear Systems*, North-Holland, Amsterdam, The Netherlands, pp. 61-70.

[5] Fraser A.R. and R.W. Daniel (1991): *Perturbation Techniques for Flexible Manipulators*, Kluwer, Boston, MA.

[6] Kelly R. and V. Santibanez (1998): "Global Regulation of Elastic Joint Robots Based on Energy Shaping", *IEEE Transactions on Automatic Control*, Vol. 43, No. 10, pp.1451-1455.

[7] Strang G. (1988): *Linear Algebra and its Applications*, Harcourt Brace Jovanovich, Inc., San Diego.

[8] Sweet L.M. and M.C. Good (1985): "Redefinition of the Robot Motion Control Problem", *IEEE Control System Magazine*, Vol. 5, No. 3, pp. 18-24.

[9] Swevers J., et.al. (1997): "Optimal Robot Excitation and Identification", *IEEE transactions on robotics and automation*, Vol. 13, No. 5, pp. 730-740.

[10] Wilson, G.A. and G.W. Irwin (1994): "Robust Tracking of Elastic Joint Manipulators Using Sliding Mode Control", *Transactions of the Institute of Measurement and Control*, Vol. 16, No. 2, pp.99-107.